

Supplementary file for

**Novel Inhibition Mechanism and NES-binding Groove Features Revealed by the
CRM1 Inhibitors Oridonin and Plumbagin**

Yuqin Lei ^{† #}, Yuling Li ^{† #}, Yuping Tan [†], Zhiyong Qian [†], Qiao Zhou [†], Da Jia [‡], Qingxiang
Sun ^{†*}

* Corresponding author: Qingxiang Sun, sunqingxiang@hotmail.com

This file includes figure S1-S11.

Supplemental Figures

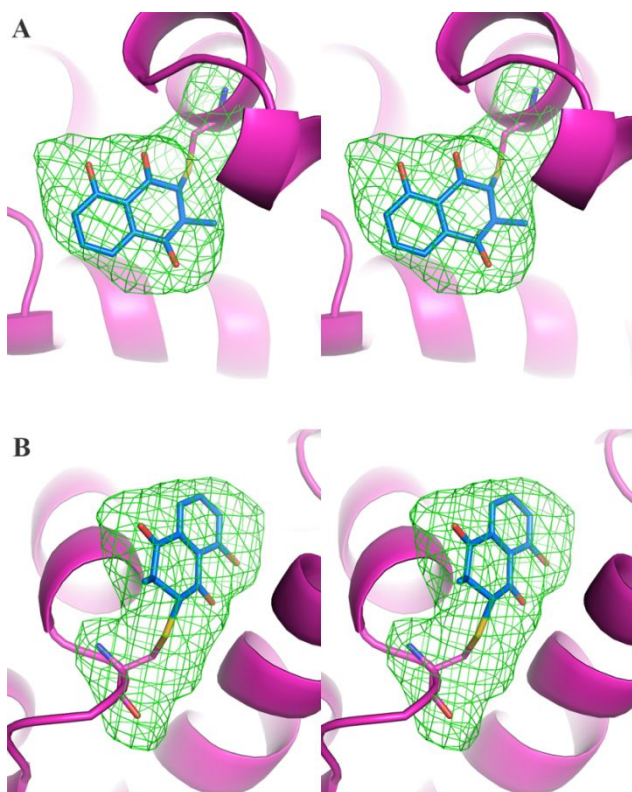


Figure S1. Stereo view of the Fo-Fc SA omit maps (green mesh) contoured at 4σ level. A) omit map for plumbagin and the conjugated cysteine C152. CRM1 is shown as magenta cartoon representation. B) omit map for plumbagin and the conjugated cysteine C1022.

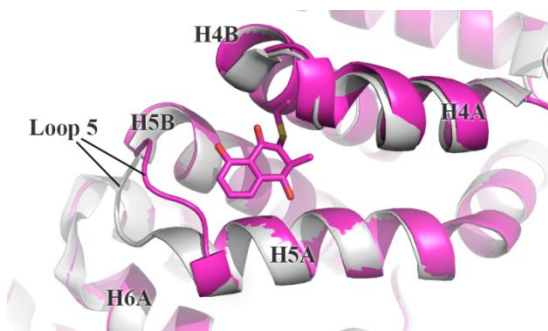


Figure S2. Comparison of C152-unliganded (4HAT, grey) and plumbagin-conjugated (magenta) CRM1 structures. Loop 5 is swung from H6 to H4 upon plumbagin binding.

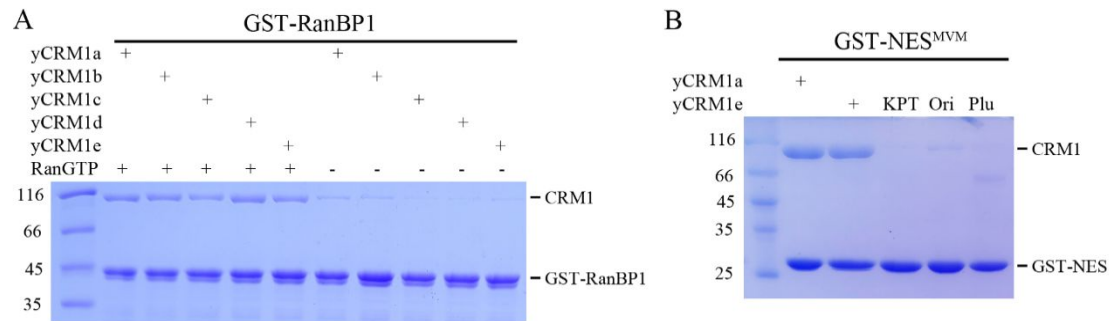


Figure S3. Analysis of CRM1 mutants in binding to RanBP1-Ran, NES, and inhibitors. A) GST-RanBP1 pull down of different CRM1 (1 μ M) constructs in the presence or absence of RanGTP (1 μ M). The binding in the absence of RanGTP represents non-specific binding which is caused by denatured proteins. B) GST-NES pull down of different CRM1 (1 μ M) constructs in the presence or absence of inhibitors (20 μ M). KPT: KPT-330.

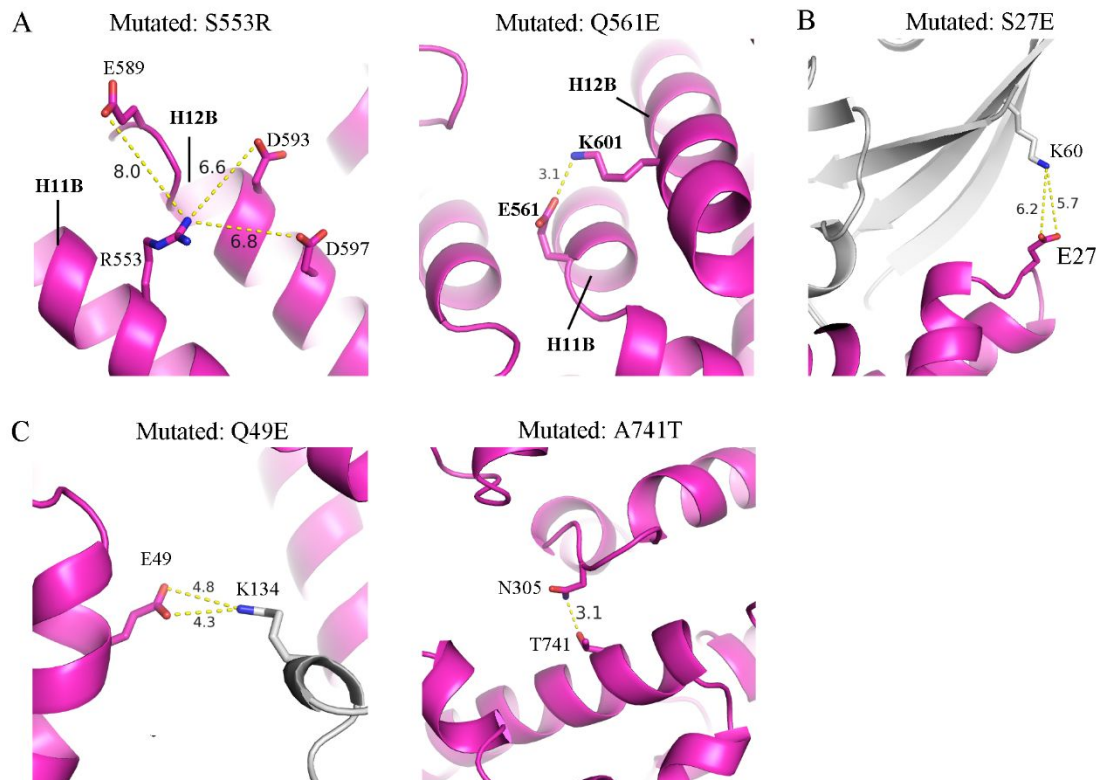


Figure S4. Conformation of mutated residues in the plumbagin-yCRM1e complex. A) residues mutated to open the NES-binding groove. Inter-atomic distances are labelled as dotted lines. B) Residue mutated to improve Ran-CRM1 affinity. C) Residues mutated to improve packing.

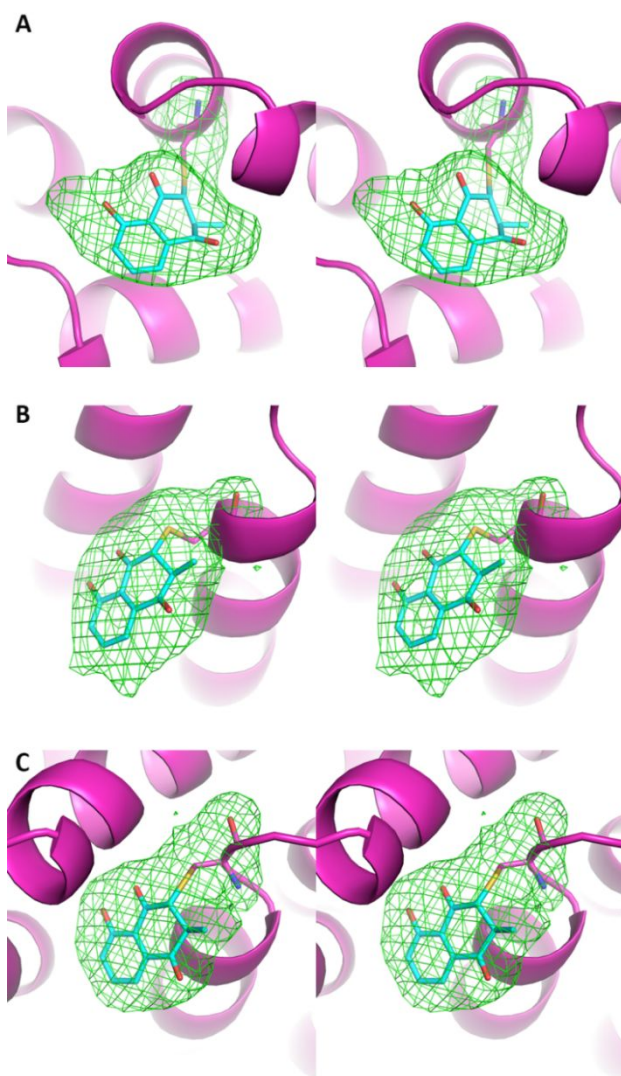


Figure S5. Stereo view of the Fo-Fc SA omit maps (green mesh) contoured at 4σ level. A) omit map for plumbagin and the conjugated cysteine C152. CRM1 is shown as magenta cartoon representation. Plumbagin is shown as cyan sticks. B) omit map for plumbagin and the conjugated C539. C) omit map for plumbagin and the conjugated C1022.

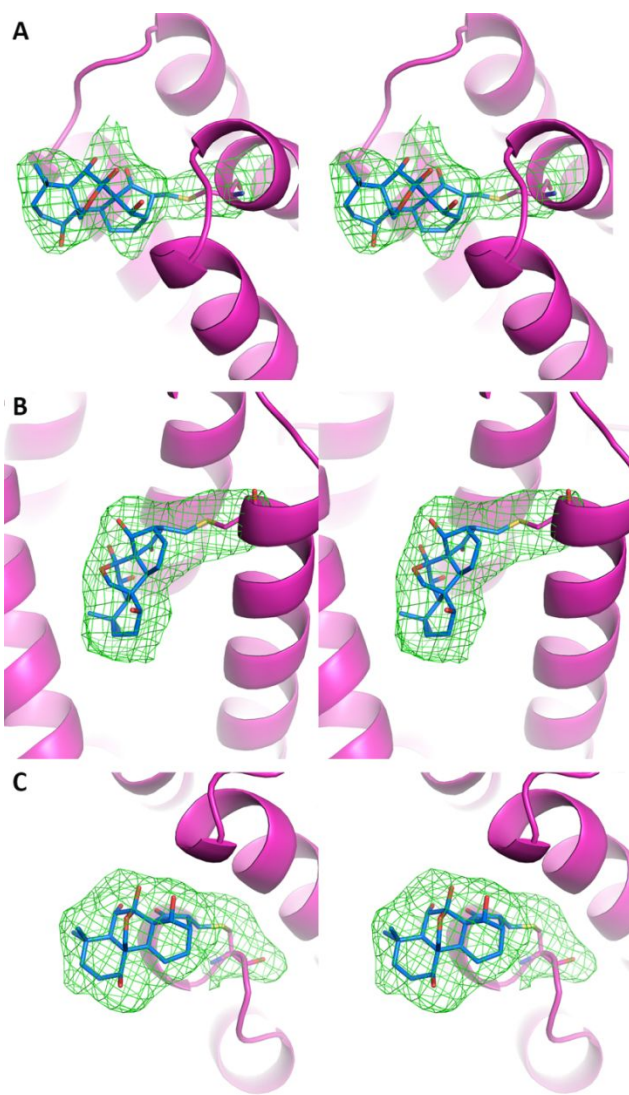


Figure S6. Stereo view of the Fo-Fc SA omit maps (green mesh) contoured at 4σ level. A) omit map for oridonin and the conjugated cysteine C152. CRM1 is shown as magenta cartoon representation. Oridonin is shown as cyan sticks. B) omit map for oridonin and the conjugated C539. C) omit map for oridonin and the conjugated C1022.

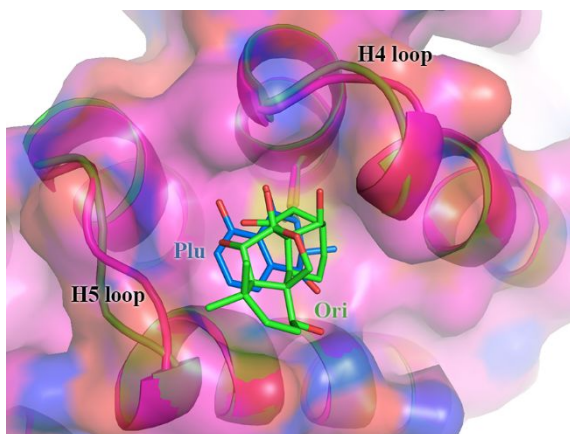


Figure S7. Overlay of C152-bound oridonin (green) and C152-bound plumbagin (blue, as in yCRM1a). Some differences of H4 and H5 loops are observed.

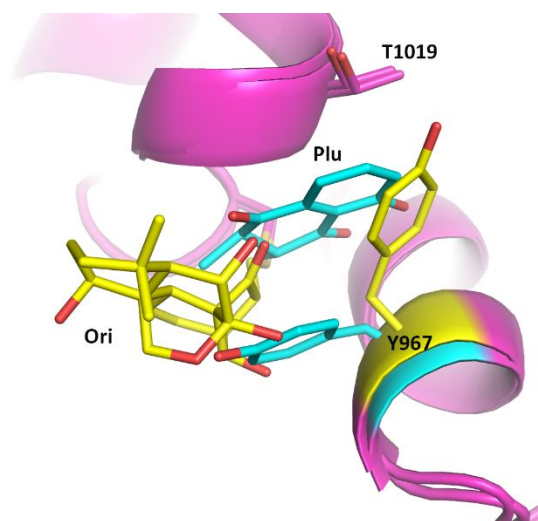


Figure S8. Comparison of C1022-linked plumbagin and oridonin. Oridonin is not inserted into the plumbagin-binding channel formed by Y967 and T1019. In oridonin complex, Y967 shifts and touches T1019, closing the plumbagin-binding channel.

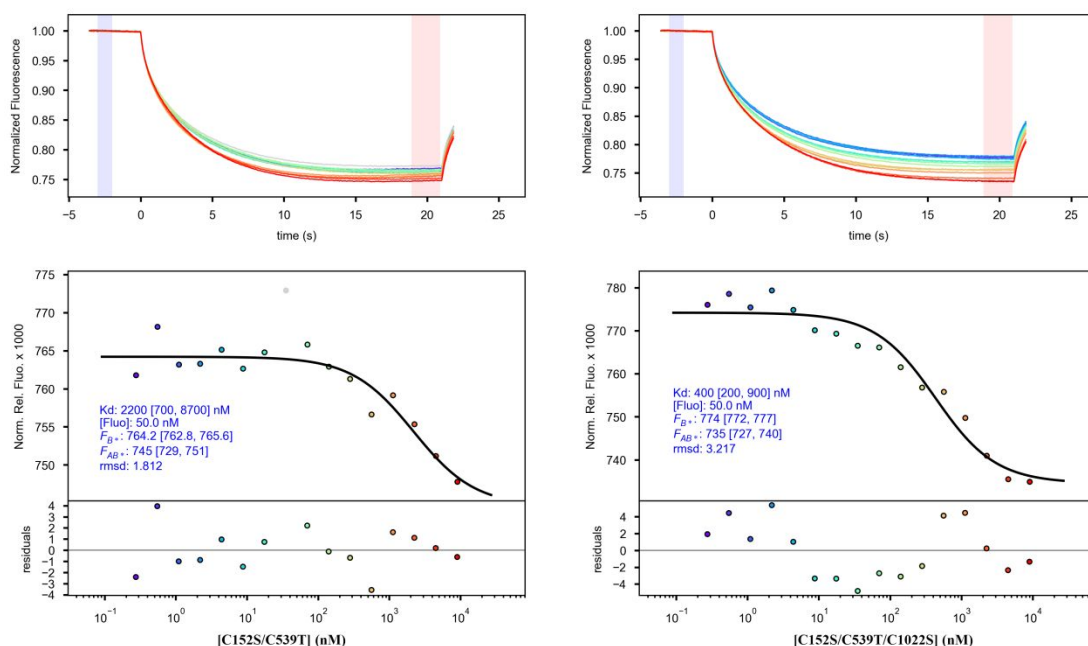


Figure S9. Microscale thermophoresis data of C152S/C539T double mutant or C152S/C539T/C1022S triple mutant binding to MBP-NES^{MVM} in the presence of excess (60 μ M) oridonin. The data is processed using the PALMIST programme. MBP-NES^{MVM} was labelled with RED-NHS dye and kept at a constant concentration of 50 nM. The LED power and MST power are 25% and 40% respectively. The assay buffer contains 50 mM Hepes pH 7.5, 200 mM NaCl, 0.05% Tween-20.

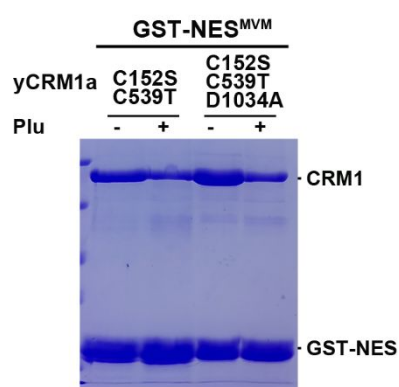


Figure S10. GST-NES^{MVM} pull down of two CRM1 mutants in the absence or presence of 25 μ M plumbagin. This experiment is performed the same as in Figure 5C, but with a different small molecule, plumbagin.

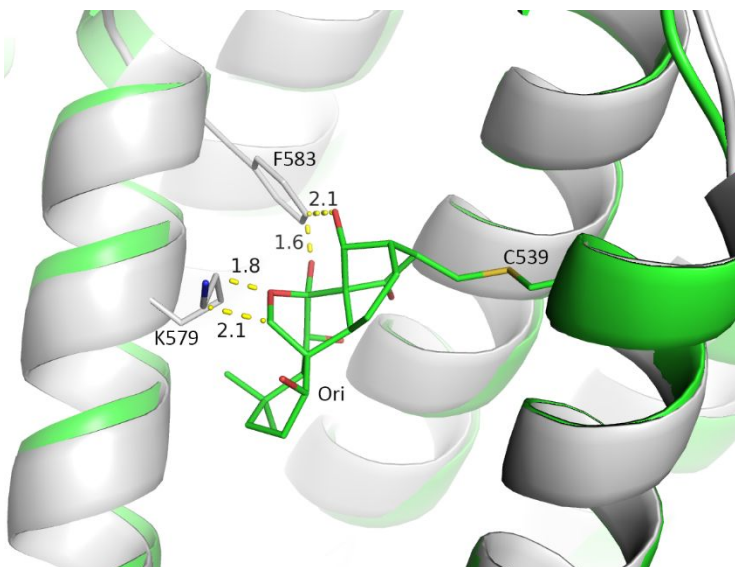


Figure S11. Alignment of NES-bound groove (grey, 6CIT) with CRM1e (green) using the H11A residues (529-540). Ordonin clashes (yellow dash lines) with F583 and K579 on H12A in the NES-bound structure.